1.0

1.1

1.25

4.5
5.0
5.6

2.8

2.5

3.2

2.2

3.6

4.0

2.0

1.8

1.4

1.6

MICROCOPY RESOLUTION TEST CHART

(12) **LEVEL** II

AD A089769

THEORY OF FREE ELECTRON LASER INSTABILITY IN A RELATIVISTIC ANNULAR ELECTRON BEAM

HAN S. UHM AND RONALD C. DAVIDSON

DTIC
S ELECTE D
OCT 1 1980
B

SCIENCE
APPLICATIONS
INCORPORATED

PLASMA RESEARCH INSTITUTE
BOULDER, COLORADO

DDC FILE COPY

80 10 1 005

SECURITY CLASSIFICATION OF THIS PAGE (When Data Entered)

REPORT DOCUMENTATION PAGE		READ INSTRUCTIONS BEFORE COMPLETING FORM
1. REPORT NUMBER SAI-254-80-494-LJ PRI 13	2. GOVT ACCESSION NO. AD-A089769	3. RECIPIENT'S CATALOG NUMBER
4. TITLE (and Subtitle) THEORY OF FREE ELECTRON LASER INSTABILITY IN A RELATIVISTIC ANNULAR ELECTRON BEAM		5. TYPE OF REPORT & PERIOD COVERED TECHNICAL REPORT
		6. PERFORMING ORG. REPORT NUMBER PRI-13
7. AUTHOR(s) HAN S. UHM* AND RONALD C. DAVIDSON** *NAVAL SURFACE WEAPONS CTR., SILVER SPRINGS, MD **PLASMA FUSION CTR., MIT		8. CONTRACT OR GRANT NUMBER(s) N00014-79-C-0555
9. PERFORMING ORGANIZATION NAME AND ADDRESS SCIENCE APPLICATIONS, INC. PLASMA RESEARCH INSTITUTE 934 PEARL STREET, BOULDER, COLORADO 80302		10. PROGRAM ELEMENT, PROJECT, TASK AREA & WORK UNIT NUMBERS
11. CONTROLLING OFFICE NAME AND ADDRESS OFFICE OF NAVAL RESEARCH PHYSICS PROGRAM OFFICE ARLINGTON, VA 22217		12. REPORT DATE AUG 80
		13. NUMBER OF PAGES 47
14. MONITORING AGENCY NAME & ADDRESS(If different from Controlling Office) 50		15. SECURITY CLASS. (of this report) UNCLASSIFIED
		15a. DECLASSIFICATION/DOWNGRADING SCHEDULE

16. DISTRIBUTION STATEMENT (of this Report)

APPROVED FOR PUBLIC RELEASE: DISTRIBUTION UNLIMITED

17. DISTRIBUTION STATEMENT (of the abstract entered in Block 20, if different from Report)

18. SUPPLEMENTARY NOTES

19. KEY WORDS (Continue on reverse side if necessary and identify by block number)

RELATIVISTIC ELECTRON BEAM FOR FREE ELECTRON LASER

20. ABSTRACT (Continue on reverse side if necessary and identify by block number)

A self-consistent theory of the free electron laser instability is developed for a hollow electron beam propagating through an undulator (multiple mirror) magnetic field. The stability analysis is carried out within the framework of the linearized Vlasov-Maxwell equations. It is assumed that the beam is

DD FORM 1473 EDITION OF 1 NOV 65 IS OBSOLETE
S/N 0102-LF-014-6601

thin, with radial thickness much smaller than the mean beam radius, and that $\nu/\gamma_b \ll 1$, where ν is Budker's parameter and $\gamma_b mc^2$ is the characteristic energy of the electron beam. The dispersion relation describing the free electron laser instability in a hollow relativistic electron beam is obtained for an equilibrium distribution function in which all electrons have same value of transverse energy and the same value of canonical angular momentum, and a Lorentian distribution in axial momentum. It is shown that the influence of finite radial geometry plays a critical role in determining detailed stability behavior. Moreover, the growth rate and bandwidth of the instability can be expressed in terms of Budker's parameter ν, instead of the plasma frequency as in the case of a uniform density beam. Furthermore, it is found that free electron laser stability properties exhibit a sensitive dependence on axial momentum spread.

$\nu \quad \nu \quad \nu \quad \mu$

ν

THEORY OF FREE ELECTRON LASER INSTABILITY IN A RELATIVISTIC

ANNULAR ELECTRON BEAM

Han S. Uhm
Naval Surface Weapons Center
White Oak, Silver Spring, Md. 20910

Ronald C. Davidson
Plasma Fusion Center
Massachusetts Institute of Technology
Cambridge, Mass. 02139

and

Science Applications Inc.
Boulder, Colorado 80302

A self-consistent theory of the free electron laser instability is developed for a hollow electron beam propagating through an undulator (multiple mirror) magnetic field. The stability analysis is carried out within the framework of the linearized Vlasov-Maxwell equations. It is assumed that the beam is thin, with radial thickness much smaller than the mean beam radius, and that $\nu/\gamma_b \ll 1$, where ν is Budker's parameter and $\gamma_b mc^2$ is the characteristic energy of the electron beam. The dispersion relation describing the free electron laser instability in a hollow relativistic electron beam is obtained for an equilibrium distribution function in which all electrons have same value of transverse energy and the same value of canonical angular momentum, and a Lorentian distribution in axial momentum. It is shown that the influence of finite radial geometry plays a critical role in determining detailed stability behavior. Moreover, the growth rate and bandwidth of the instability can be expressed in terms of Budker's parameter ν, instead of the plasma frequency as in the case of a uniform density beam. Furthermore, it is found that free electron laser stability properties exhibit a sensitive dependence on axial momentum spread.

I. INTRODUCTION

In recent years, there has been a growing interest in the free electron laser instability[1-7] in connection with intense radiation generation.[8-10] For the most part, previous theoretical analyses of this instability have been carried out for an electron beam with uniform density, neglecting the influence of finite radial geometry. Although this is a reasonable first approach to the problem, for detailed application to present experiments it is necessary to investigate the important influence of finite radial geometry on stability properties. In this regard, in the present analysis we investigate free electron laser stability properties for an annular electron beam propagating through an undulator (multiple mirror) wiggler field, including the full influence of finite radial geometry.

Equilibrium and stability properties are calculated for the choice of equilibrium beam distribution function [Eq. (19)]

$$f_b^0(H, P_\theta, p_z) = K\delta(P_\theta - P_0)F(p_\perp^2)G(p_z),$$

where H is the energy, P_θ is the canonical angular momentum, $p_\perp = (p_r^2 + p_\theta^2)^{1/2}$ is the transverse momentum, p_z is the axial momentum, and K is a normalization constant. The present analysis is carried out within the framework of the linearized Vlasov-Maxwell equations, assuming that the beam thickness is much less than the mean beam radius R_0, and that $\nu/\gamma_b \ll 1$, where ν is Budker's parameter. It is also assumed that the electron beam propagates through an undulator (multiple mirror) magnetic field and that the amplitude $\hat{B}$ of the wiggler field is small in comparison with the average field B_0.

The basic assumptions and equilibrium properties are discussed in Sec. II. The formal stability analysis for azimuthally symmetric perturbations ($\partial/\partial\theta = 0$) is carried out in Sec. III for general transverse and longitudinal distribution functions, $F(p_\perp^2)$ and $G(p_z)$. The matrix eigenvalue equation (65), when combined with Eq. (67), constitutes one of the main results of this paper and can be used to investigate stability properties for a broad range of distribution functions corresponding to a thin annular electron beam.

In Sec. IV, the dispersion relation for the free electron laser instability is obtained for the specific choice of equilibrium distribution function in which all electrons have the same value of transverse momentum, and a Lorentzian distribution in axial momentum [Eq. (69)]

$$G(p_z) = \frac{\Delta}{\pi} \frac{1}{(p_z - p_b)^2 + \Delta^2} .$$

Here, Δ is the characteristic axial momentum spread about the mean value $p_b = \gamma_b m V_b$. One of the most important consequences of finite radial geometry is the fact that the maximum instability growth rate occurs for a value of beam radius R_0 satisfying [Eq. (97)]

$$R_0/R_c = \beta_{0\ell}/\alpha_{0s} ,$$

where R_c is the radius of outer conducting wall, $\beta_{0\ell}$ is the ℓth root of $J_0(\beta_{0\ell}) = 0$, and α_{0s} is the sth root of $J_1(\alpha_{0s}) = 0$. Moreover, the growth rate and instability bandwidth can be expressed in terms of Budker's parameter ν and the amplitude of the wiggler field $\hat{B}$. It is found that the maximum growth rate increases with increasing beam intensity (ν).

The dependence of stability properties on the axial momentum spread (Δ) is also investigated in Sec. IV. It is shown that the maximum growth rate of the instability decreases as the axial momentum spread Δ is increased. However, the instability bandwidth increases with increasing Δ. We conclude that free electron laser stability properties exhibit a sensitive dependence on axial momentum spread Δ.

II. EQUILIBRIUM CONFIGURATION AND BASIC ASSUMPTIONS

A. Basic Assumptions

The present analysis assumes an intense annular electron beam with characteristic thickness 2a and mean radius R_0 propagating in the z-direction (Fig. 1). We introduce a cylindrical polar coordinate system (r,θ,z) with z-axis along the axis of symmetry; r is the radial distance from the axis of symmetry, and θ is the polar angle in a plane perpendicular to the z-axis. To make the analysis tractable, the following simplifying assumptions are made.

(a) The thickness of the annular electron beam is much smaller than its mean radius, i.e.,

$$a/R_0 \ll 1. \tag{1}$$

. (b) It is assumed that the beam density and current are sufficiently small that equilibrium space charge effects are negligibly small, and the equilibrium self magnetic field can be neglected in comparison with the applied magnetic field $\underset{\sim}{B}^0$. That is, we approximate:

$$\underset{\sim s}{E}^0 = 0 = \underset{\sim s}{B}^0 , \tag{2}$$

where $\underset{\sim s}{E}^0$ and $\underset{\sim s}{B}^0$ are the equilibrium electric and magnetic self fields, respectively.

(c) Consistent with Assumption (b), it is assumed that

$$\nu/\gamma_b \ll 1, \tag{3}$$

where $\gamma_b mc^2$ is the characteristic electron energy, and $\nu = N_b e^2/mc^2$

is Budker's parameter. Here, $-e$ is the electron charge, c is the speed of light in vacuo, m is the electron rest mass, and $N_b = 2\pi \int_0^\infty dr\; r\; n_b^0 (r,z)$ is the number of electrons per unit axial length. For a thin annular electron beam with radial thickness $2a$ and constant density n_0, the inequality in Eq. (3) can be expressed in the equivalent form

$$\hat{\omega}_p R_0^2 / c^2 \ll R_0/a, \qquad (4)$$

where $\hat{\omega}_p^2 = 4\pi n_0 e^2 / \gamma_b m$ is the relativistic plasma frequency-squared.

(d) It is assumed that the electron beam propagates through an undulator (multiple mirror) magnetic field. The azimuthal component of vector potential $A_\theta^0(r,z)$ for the equilibrium magnetic field can be expressed as

$$A_\theta^0(r,z) = \frac{1}{2} B_0 \left(r - \frac{2}{k_0} \; \frac{R-1}{R+1} \; I_1(k_0 r)\cos k_0 z \right), \qquad (5)$$

where $\lambda_0 = 2\pi/k_0$ is the periodicity length, $I_1(x)$ is the modified Bessel function of the first kind of order unity, and $R = B_{0z}(r = 0, k_0 z = \pm\pi)/B_{0z}(r = 0, k_0 z = 0)$ is the mirror ratio. Here, the equilibrium magnetic field components are given by $B_{0r} = -\partial A_\theta^0/\partial z$ and $B_{0z} = r^{-1}(\partial/\partial r)(r A_\theta^0)$.

(e) We further assume that

$$k_0 a \ll 1 \qquad (6)$$

where a is the half-thickness of the annular beam. Defining the characteristic wiggler amplitude by

$$\frac{\hat{B}}{B_0} = 2 \; \frac{R-1}{R+1} \; \frac{I_1(k_0 R_0)}{k_0 R_0} \; ,$$

the equilibrium vector potential [Eq. (5)] can be expressed in the equivalent form

$$A_\theta^0(r,z) = \frac{1}{2} B_0 r \left[1 - \frac{\hat{B}}{B_0} \frac{R_0}{r} \frac{I_1(k_0 r)}{I_1(k_0 R_0)} \cos k_0 z \right].$$ (7)

From Eq. (7), the components of the equilibrium magnetic field $\underset{\sim}{B}^0 = B_{0r}\hat{\underset{\sim}{e}}_r + B_{0z}\hat{\underset{\sim}{e}}_z$ are given by

$$\begin{aligned} B_{0r}(r,z) &= -\frac{\partial}{\partial z} A_\theta^0(r,z) \\ &= -\frac{1}{2} k_0 R_0 \hat{B} \frac{I_1(k_0 r)}{I_1(k_0 R_0)} \sin k_0 z \\ &\simeq -\hat{B}_r \sin k_0 z, \end{aligned}$$ (8)

where

$$\hat{B}_r = \frac{1}{2} k_0 R_0 \hat{B} = B_0 \frac{R-1}{R+1} I_1(k_0 R_0),$$

and

$$\begin{aligned} B_{0z}(r,z) &= \frac{1}{r} \frac{\partial}{\partial r} [r A_\theta^0(r,z)] \\ &= B_0 - \frac{1}{2} \hat{B} k_0 R_0 \frac{I_0(k_0 r)}{I_1(k_0 R_0)} \cos k_0 z \\ &\simeq B_0 \left(1 - \frac{\hat{B}_z}{B_0} \cos k_0 z \right), \end{aligned}$$ (9)

where

$$\hat{B}_z = \frac{1}{2} k_0 R_0 \hat{B} \frac{I_0(k_0 R_0)}{I_1(k_0 R_0)} = B_0 \frac{R-1}{R+1} I_0(k_0 R_0).$$

Note from Eq. (9) that B_0 is equal to the average axial magnetic field (averaged over the periodicity length $\lambda_0 = 2\pi/k_0$). Note also that the approximate expressions for B_{0r} and B_{0z} given in Eqs. (8) and (9) are valid over the radial extent of the beam ($R_0 - a < r < R_0 + a$) within the context of the assumption that $k_0 a \ll 1$ [Eq. (6)]

(f) From Eq. (9), there is an oscillatory (wiggler) contribution to the axial magnetic field proportional to $- (\hat{B}_z/B_0) \cos k_0 z$. Throughout the present analysis, it is assumed that the amplitude of the wiggler field is small, i.e.,

$$\frac{\hat{B}_z}{B_0} \ll 1 . \tag{10}$$

The inequality in Eq. (10) assures that the axial modulation of the equilibrium beam envelope is small. Equally important, Eqs. (1) and (10) assure that the axial momentum $p_z = \gamma m v_z$, where $\gamma = (1 + p^2/m^2 c^2)^{1/2}$, is a good approximate single-particle invariant to lowest order. In Appendix A, we present a detailed investigation of the electron trajectories in the equilibrium fields described by Eqs. (2), (8), and (9), assuming that the axial motion is non-resonant with

$$k_0^2 v_z^2 \neq \omega_c^2 . \tag{11}$$

Here $v_z = p_z/\gamma m$ is the axial velocity of a typical beam electron, and $\omega_c = eB_0/\gamma mc$ is the relativistic electron cyclotron frequency. For example, in the strong-magnetic-field limit $(\omega_c^2 \gg k_0^2 v_z^2)$, it is shown in Appendix A that $p_z \simeq$ const. whenever the inequalities [Eqs. (A.20) and (A.21)]

$$\frac{1}{2} \frac{a}{R_0} \frac{\hat{B}}{B_0} (k_0 R_0) \left(\frac{\omega_c R_0}{v_z} \right) \ll 1 , \tag{12}$$

and

$$\frac{1}{4} \frac{\hat{B}^2}{B_0^2} (k_0 R_0) \left(\frac{\omega_c R_0}{v_z} \right) \ll 1 , \tag{13}$$

are satisfied. From Eqs. (1) and (10), the inequalities in Eqs. (12) and (13) are straightforward to satisfy in the parameter regimes of experimental interest.

(g) Finally, in the stability analysis (Sec. III), it is assumed that the waves are close to resonance with

$$\left| \omega - (k + nk_0)V_b \right| \ll k_0 V_b, \; \omega_c, \tag{14}$$

where ω is the complex oscillation frequency, $k + nk_0$ is the excited wavenumber, and $V_b = \int d^3 p v_z f_b^0$ is the mean axial velocity of the electron beam.

In summary, the present equilibrium and stability analysis is carried out within the context of the inequalities in Eqs. (1), (2), (4), (6), and (10) – (14). Moreover, the vector potential for the equilibrium magnetic field is approximated by Eq. (7).

B. General Equilibrium Properties

Within the context of Assumptions (b), (e), and (f) in Sec. II.A, the equilibrium $(\partial/\partial t = 0)$ beam distribution $f_b^0(r,z,\underset{\sim}{p})$ is generally a function of the single-particle invariants[11] corresponding to particle energy,

$$H = (m^2 c^4 + c^2 \underset{\sim}{p}^2)^{1/2} , \tag{15}$$

canonical angular momentum,

$$P_\theta = r[p_\theta - \frac{e}{c} A_\theta^0(r,z)] , \tag{16}$$

and axial momentum

$$P_z \tag{17}$$

where $A_\theta^0(r,z)$ is defined in Eq. (7), and $\underset{\sim}{p} = (p_r, p_\theta, p_z)$ is the mechanical momentum. In Eqs. (15) – (17), we have neglected

equilibrium self-field effects and assumed that the wiggler amplitude $\hat{B}$ is sufficiently small [Eqs. (10), (12), and (13)] that p_z is an approximate invariant. In this regard, we also conclude that the transverse momentum

$$p_\perp = (H^2/c^2 - m^2c^2 - p_z^2)^{1/2} , \tag{18}$$

is also an approximate invariant. Here, the particle velocity $\underset{\sim}{v}$ is related to the momentum $\underset{\sim}{p}$ by $\underset{\sim}{v} = \underset{\sim}{p}/\gamma m$ where $\gamma = H/mc^2 = (1 + p_{\sim}^2/m^2c^2)^{1/2}$ is the relativistic mass factor.

In the present analysis, we consider the general class of annular electron beam equilibria described by[11]

$$f_b^0(r,z,\underset{\sim}{p}) = K\delta(P_\theta - P_0)F(p_\perp^2)G(p_z) , \tag{19}$$

where K is a positive normalization constant, P_0 = const. is defined by

$$P_0 = -\frac{1}{2}\frac{eB_0}{c}R_0^2 , \tag{20}$$

and the transverse and longitudinal momentum distribution functions are normalized according to

$$\int_0^\infty dp_\perp^2 \, F(p_\perp^2) = 1 , \quad \int_{-\infty}^\infty dp_z \, G(p_z) = 1. \tag{21}$$

Defining $r_L = cp_\perp/eB_0$, and carrying out some straightforward algebraic manipulation,[11] the electron distribution function in Eq. (19) can be expressed in the equivalent form

$$f_b^0(r,z,\underset{\sim}{p}) = \frac{N_b}{\pi^2} F(p_\perp^2)G(p_z) \frac{\Theta[(r-r_1)(r_2-r)]}{[(r^2-r_1^2)(r_2^2-r^2)]^{1/2}}$$

$$\times [\delta(\hat{\phi} - \hat{\phi}_0) + \delta(\hat{\phi} - \pi + \hat{\phi}_0)] , \tag{22}$$

where $\hat{\phi} = \sin^{-1}(p_\theta/p_\perp)$, and (for $\hat{B}_z/B_0 \ll 1$) the quantities r_1, r_2 and $\hat{\phi}_0$ can be approximated by

$$r_1(z) = \left[\frac{R_0^2}{\left(1 - \frac{\hat{B}}{B_0} \cos k_0 z\right)} + \frac{r_L^2}{\left(1 - \frac{\hat{B}}{B_0} \cos k_0 z\right)^2} \right]^{1/2} - \frac{r_L}{\left(1 - \frac{\hat{B}}{B_0} \cos k_0 z\right)} ,$$

(23)

$$r_2(z) = r_1(z) + \frac{2r_L}{\left(1 - \frac{\hat{B}}{B_0} \cos k_0 z\right)} ,$$

(24)

and

$$\hat{\phi}_0 = \sin^{-1} \left(\frac{r^2 \left(1 - \frac{\hat{B}}{B_0} \cos k_0 z\right) - R_0^2}{2 r r_L} \right) . \, .$$

(25)

In Eq. (22), $\Theta(x)$ is the Heaviside step function defined by

$$\Theta(x) = \begin{cases} 1 , & x > 0 , \\ 0 , & x < 0 , \end{cases}$$

(26)

and N_b is the number of electrons per unit axial length defined by

$$N_b = 2\pi \int_0^{R_c} dr\, r \int_0^{2\pi} d\hat{\phi} \int_0^\infty dp_\perp p_\perp \int_{-\infty}^\infty dp_z\, f_b^0(r, z, \underline{p}) .$$

(27)

Here, R_c is the radius of the grounded cylindrical conducting wall. Several equilibrium examples of the general form given by Eq. (22) have been discussed previously in the literature[11] in the absence of wiggler field ($\hat{B}=0$).

III. LINEARIZED VLASOV-MAXWELL EQUATIONS

A. General Formulation

In this section, we develop the general formalism to investigate stability properties for perturbations about the class of beam equilibria described by Eqs. (19) and (22). Expressing the beam distribution function as $f_b(\underset{\sim}{x}, \underset{\sim}{p}, t) = f_b^0 + \delta f_b(\underset{\sim}{x}, \underset{\sim}{p}, t)$, and neglecting equilibrium self-field effects [Sec. II.A], the linearized Vlasov equation can be expressed as

$$\left\{ \frac{\partial}{\partial t} + \underset{\sim}{v} \cdot \frac{\partial}{\partial \underset{\sim}{x}} - e \frac{\underset{\sim}{v} \times \underset{\sim}{B}^0}{c} \cdot \frac{\partial}{\partial \underset{\sim}{p}} \right\} \delta f_b(\underset{\sim}{x}, \underset{\sim}{p}, t)$$

$$= e \left(-\nabla \delta \phi - \frac{1}{c} \frac{\partial}{\partial t} \delta \underset{\sim}{A} + \frac{\underset{\sim}{v} \times \underset{\sim}{\nabla} \times \delta \underset{\sim}{A}}{c} \right) \cdot \frac{\partial}{\partial \underset{\sim}{p}} f_b^0(r, z, \underset{\sim}{p}) \ , \tag{28}$$

where $\underset{\sim}{v} = \underset{\sim}{p}/\gamma m$ is the particle velocity, the equilibrium magnetic field components $\underset{\sim}{B}^0 = B_{0r}\hat{\underset{\sim}{e}}_r + B_{0z}\hat{\underset{\sim}{e}}_z$ are given in Eqs. (8) and (9), and use has been made of the Lorentz gauge to express the perturbed magnetic field as $\delta \underset{\sim}{B}(\underset{\sim}{x}, t) = \underset{\sim}{\nabla} \times \delta \underset{\sim}{A}(\underset{\sim}{x}, t)$, and the perturbed electric field as $\delta \underset{\sim}{E}(\underset{\sim}{x}, t) = -\nabla \delta \phi(\underset{\sim}{x}, t) - (1/c)(\partial/\partial t) \delta \underset{\sim}{A}(\underset{\sim}{x}, t)$, where $\underset{\sim}{\nabla} \cdot \delta \underset{\sim}{A}(\underset{\sim}{x}, t) + (1/c)(\partial/\partial t)\delta \phi(\underset{\sim}{x}, t) = 0$. The corresponding linearized Maxwell equations that determine the evolution of $\delta \underset{\sim}{A}$ and $\delta \phi$ self-consistently are given by

$$\left(\frac{1}{c^2} \frac{\partial^2}{\partial t^2} - \nabla^2 \right) \delta \underset{\sim}{A} = -\frac{4\pi e}{c} \int d^3p \ \underset{\sim}{v} \ \delta f_b \ , \tag{29}$$

and

$$\left(\frac{1}{c^2} \frac{\partial^2}{\partial t^2} - \nabla^2 \right) \delta \phi = -4\pi e \int d^3p \ \delta f_b \ , \tag{30}$$

where the perturbed current $-e\int d^3p \ \underset{\sim}{v} \ \delta f_b$ and perturbed charge density $-e\int d^3p \delta f_b$ are calculated from Eq. (28). In the present analysis, we assume azimuthally symmetric perturbations with

$$\partial/\partial\theta = 0 \ , \tag{31}$$

but $\partial/\partial z$ and $\partial/\partial r$ generally non-zero. The components of the perturbed magnetic and electric fields can then be expressed as

$$\delta B_r = -\frac{\partial}{\partial z} \delta A_\theta \ ,$$

$$\delta B_\theta = \frac{\partial}{\partial z} \delta A_r - \frac{\partial}{\partial r} \delta A_z \ , \tag{32}$$

$$\delta B_z = \frac{1}{r}\frac{\partial}{\partial r} (r\delta A_\theta) \ ,$$

and

$$\delta E_r = -\frac{\partial}{\partial r} \delta\phi - \frac{1}{c}\frac{\partial}{\partial t} \delta A_r \ ,$$

$$\delta E_\theta = -\frac{1}{c}\frac{\partial}{\partial t} \delta A_\theta \ , \tag{33}$$

$$\delta E_z = -\frac{\partial}{\partial z} \delta\phi - \frac{1}{c}\frac{\partial}{\partial t} \delta A_z \ ,$$

and the Lorentz gauge condition $\underset{\sim}{\nabla} \cdot \delta\underset{\sim}{A} + (1/c)\partial \delta\phi/\partial t = 0$ becomes

$$\frac{1}{r}\frac{\partial}{\partial r} (r\delta A_r) + \frac{\partial}{\partial z} \delta A_z + \frac{1}{c}\frac{\partial}{\partial t} \delta\phi = 0 \ . \tag{34}$$

In the subsequent analysis, we assume that all perturbation quantities have time and spatial variations of the form

$$\delta\psi(r,z,t) = \delta\hat{\psi}(r,z)\exp(-i\omega t) \ ,$$

where $\text{Im}\,\omega > 0$, and $\delta\hat{\psi}(r,z)$ is the amplitude of the perturbation. Using the method of characteristics, the linearized Vlasov equation (28) can be integrated to give

$$\delta f_b(\underset{\sim}{x},\underset{\sim}{p},t) = e \int_{-\infty}^{t} dt' \left[-\nabla'\delta\phi(\underset{\sim}{x}',t') - \frac{1}{c}\frac{\partial}{\partial t'}\, \delta\underset{\sim}{A}(\underset{\sim}{x}',t') \right.$$

$$\left. + \frac{\underset{\sim}{v}' \times \underset{\sim}{v}' \times \delta\underset{\sim}{A}(\underset{\sim}{x}',t')}{c} \right] \cdot \frac{\partial}{\partial \underset{\sim}{p}'}\, f_b^0(\underset{\sim}{x}',\underset{\sim}{p}') \ , \tag{35}$$

where $d\underset{\sim}{x}'/dt' = \underset{\sim}{v}'$ and $d\underset{\sim}{p}'/dt' = -e\underset{\sim}{v}' \times \underset{\sim}{B}^0(\underset{\sim}{x}')/c$, and the particle trajectories $(\underset{\sim}{x}',\underset{\sim}{p}')$ in the equilibrium field configuration satisfy the "initial" conditions $\underset{\sim}{x}'(t' = t) = \underset{\sim}{x}$ and $\underset{\sim}{p}'(t' = t) = \underset{\sim}{p}$ (Appendix A).

We now simplify the right-hand side of Eq. (35). Without loss of generality, the perturbation amplitudes are expanded according to

$$\delta\hat{\phi}(r,z) = \sum_n \phi_n(r)\exp[i(k+nk_0)z] \ , \tag{36}$$

etc. The particle orbits $(\underset{\sim}{x}',\underset{\sim}{p}')$ are calculated in detail in Appendix A for the case of small wiggler amplitude $(\hat{B}_z/B_0 \ll 1)$ assuming that the axial and cyclotron motions are far removed from cyclotron resonance [Eq. (11)], i.e.,

$$k_0^2 v_z^2 \neq \omega_c^2 \ ,$$

where $v_z = p_z/\gamma m$ is the axial velocity and $\omega_c = eB_0/\gamma mc$ is the relativistic cyclotron frequency. To lowest order, the axial motion is free-streaming [Eq. (A.8)]

$$z' = z + \frac{p_z}{\gamma m}\,(t' - t) \ , \tag{37}$$

and the radial orbit [Eq. (A.13)] and azimuthal orbit [Eq. (A.17)] contain oscillatory contributions proportional to $\cos\omega_c\tau$, $\sin\omega_c\tau$, $\sin(k_0 z + k_0 v_z\tau)$ and $\cos(k_0 z + k_0 v_z\tau)$, where $\tau = t' - t$. For present purposes, in the t' - integration on the right-hand side of Eq. (35), we retain terms proportional to

$$[\omega - (k + nk_0)p_z/\gamma m]^{-1} \ ,$$

and assume that the value of $[\omega - (k + nk_0)p_z/\gamma m]$ is well removed

from resonance with the cyclotron motion and the beam motion [Eq. (14)], i.e.,

$$\left|\omega - (k + nk_0)p_z/\gamma m\right| \ll \omega_c \, , \quad k_0 v_b \, .$$

Within the context of Eqs. (1) and (14), Eq. (35) can be approximated by

$$\delta\hat{f}_b(\underset{\sim}{x},\underset{\sim}{p}) = -e \int_{-\infty}^{0} d\tau \exp(-i\omega\tau) \left\{ 2\left[\gamma m i \omega \left(\delta\hat{\phi} - \frac{1}{c} \underset{\sim}{v}' \cdot \delta\hat{A}\right)\right.\right.$$

$$\left.- p_z \left(\frac{\partial}{\partial z} \delta\hat{\phi} - \frac{1}{c} \underset{\sim}{v}' \cdot \frac{\partial}{\partial z} \delta\hat{A}\right)\right] \frac{\partial f_b^0}{\partial p_\perp^2} + \left(\frac{\partial}{\partial z} \delta\hat{\phi} - \frac{1}{c} \underset{\sim}{v}' \cdot \frac{\partial}{\partial z} \delta\hat{A}\right) \quad (38)$$

$$\left. \cdot \frac{\partial f_b^0}{\partial p_z} \right\} \, ,$$

where $\gamma = H/mc^2 = (1 + p^2/m^2c^2)^{1/2}$. Moreover, within the context of

Eq. (14), only those contributions to v_r' and v_θ' proportional to $\sin(k_0 z + k_0 v_z \tau)$

and $\cos(k_0 z + k_0 v_z \tau)$ are retained, i.e., on the right-hand side of

Eq. (38), we retain contributions to v_r' and v_θ' of the form

$$v_r' = -\frac{1}{2} R_0 \frac{\hat{B}}{B_0} \frac{\omega_c^2}{\omega_c^2 - k_0^2 v_z^2} k_0 v_z \sin(k_0 z + k_0 v_z \tau), \quad (39)$$

$$v_\theta' = \frac{1}{2} R_0 \frac{\hat{B}}{B_0} \frac{\omega_c^2}{\omega_c^2 - k_0^2 v_z^2} \frac{k_0^2 v_z^2}{\omega_c} \cos(k_0 z + k_0 v_z \tau) \, , \quad (40)$$

where $v_z = p_z/\gamma m$, $\omega_c = eB_0/\gamma mc$, and use has been made of Eqs. (A.13)

and (A.17). Finally, since the oscillatory modulation of the

radial orbit is small-amplitude [Eq. (A.13)], we approximate

$r' \simeq r$ in the arguments of the perturbation amplitudes on the right-

hand side of Eq. (38), i.e., $\delta\hat{\phi}(r',z') \simeq \delta\hat{\phi}(r,z')$, $\delta\hat{A}_\theta(r',z') \simeq \delta\hat{A}_\theta(r,z')$,

etc.

Substituting Eqs. (36), (37), (39), and (40) on the right-hand

side of Eq. (38), and making use of the various approximations

enumerated above, we find after some straightforward algebra that

$\delta \hat{f}_b(\chi, p)$ can be expressed as

$$\delta \hat{f}_b(\chi, p) = e \sum_n \frac{\exp[i(k + nk_0)z]}{\omega - (k + nk_0)v_z} \left\{ \lambda_n(p, \omega, k)\left(\phi_n - \frac{v_z}{c} A_{z,n}\right) \right.$$

$$- \frac{R_0}{4c} \frac{\hat{B}}{B_0} \frac{\omega_c^2}{\omega_c^2 - k_0^2 v_z^2} \frac{k_0^2 v_z^2}{\omega_c^2} \left[\lambda_{n-1}(p, \omega, k)A_{\theta, n-1} + \lambda_{n+1}(p, \omega, k)A_{\theta, n+1} \right]$$

$$\left. + \frac{iR_0}{4c} \frac{\hat{B}}{B_0} \frac{\omega_c^2}{\omega_c^2 - k_0^2 v_z^2} k_0 v_z \left[\lambda_{n+1}(p, \omega, k)A_{r, n+1} - \lambda_{n-1}(p, \omega, k)A_{r, n-1} \right] \right\}, \quad (41)$$

where the function $\lambda_{n'}(p, \omega, k)$ is defined by

$$\lambda_{n'}(p, \omega, k) = 2[\gamma m\omega - (k + n'k_0)p_z] \frac{\partial f_b^0}{\partial p_\perp^2} + (k + n'k_0) \frac{\partial f_b^0}{\partial p_z} . \quad (42)$$

Evidently, $\lambda_{n'}(p, \omega, k)$ is an even function of $v_r = p_r/\gamma m$. Therefore, it follows from Eq. (41) that

$$-e \int d^3p \ v_r \ \delta \hat{f}_b(\chi, p) = 0 . \quad (43)$$

That is, the perturbed radial current is equal to zero. The radial component of Eq. (29) then gives

$$\frac{\partial}{\partial r} \frac{1}{r} \frac{\partial}{\partial r} (rA_{r,n}) - (k + nk_0)^2 A_{r,n} + \frac{\omega^2}{c^2} A_{r,n} = 0 , \quad (44)$$

for the perturbation amplitude $A_{r,n}(r)$. Without loss of generality, for the TE mode polarization, we assume

$$A_{r,n}(r) = 0 , \quad (45)$$

in the subsequent analysis. The Lorentz gauge condition in Eq. (34) then gives the simple relation between $A_{z,n}(r)$ and $\phi_n(r)$

$$(k + nk_0)A_{z,n}(r) = \frac{\omega}{c} \phi_n(r) . \quad (46)$$

Making use of Eqs. (45) and (46), $\delta \hat{f}_b(\chi, p)$ can then be expressed as

$$\delta \hat{f}_b(\chi, \rho) = e \sum_n \frac{\exp[i(k + nk_0)z]}{\omega - (k + nk_0)v_z} \left\{ \lambda_n \left(1 - \frac{v_z}{c} \frac{\omega}{(k + nk_0)c} \right) \phi_n \right.$$

$$\left. - \frac{R_0}{4c} \frac{\hat{B}}{B_0} \frac{\omega_c^2}{\omega_c^2 - k_0^2 v_z^2} \frac{k_0^2 v_z^2}{\omega_c^2} [\lambda_{n-1} A_{\theta,n-1} + \lambda_{n+1} A_{\theta,n+1}] \right\} . \tag{47}$$

B. Eigenvalue Equations

The linearized Maxwell equations are obtained in this section within the context of Eqs. (1) and (14). For convenience in the subsequent analysis, we define the dimensionless potentials as

$$\hat{\phi}_n(r) = \frac{e}{mc^2} \left(\phi_n(r) - \frac{V_b}{c} A_{z,n}(r) \right) , \tag{48}$$

and

$$\hat{A}_n(r) = \frac{e}{mc^2} A_{\theta,n}(r) . \tag{49}$$

Moreover, we also introduce the dimensionless parameters

$$\alpha = \frac{k_0^2 v_b^2}{\omega_c^2 - k_0^2 v_b^2} , \tag{50}$$

$$\Lambda = \frac{e\hat{B}R_0}{4\gamma_b mc^2} , \tag{51}$$

and the effective susceptibility

$$\chi_{n,n'}^{(j)}(\omega,k) = 4\pi e^2 \int_0^{R_c} rdr \int d^3p \frac{\lambda_{n'}(\rho,\omega,k)(\gamma_b/\gamma)^j}{[\omega - (k + nk_0)v_z]} , \tag{52}$$

where $\lambda_{n'}(\rho,\omega,k)$ is defined in Eq. (42), and $\omega_c \equiv eB_0/\gamma_b mc$ in Eq. (50). In Eq. (51), γ_b is the relativistic mass factor defined by $\gamma_b^2 = (1 - v_b^2/c^2)^{-1}$. Noting that the azimuthal velocity at $t' = t$ is given by [Eq. (A.17)]

$$v_\theta = -(2c\gamma_b/\gamma)\Lambda \cos k_0 z , \tag{53}$$

and making use of Eqs. (42) – (52), the Maxwell equations (29) and (30) can be expressed in the approximate form,

$$\left\{\frac{1}{r}\frac{\partial}{\partial r} r \frac{\partial}{\partial r} + \frac{\omega^2}{c^2} - (k + nk_0)^2\right\}\hat{\phi}_n(r) = - \frac{\delta(r - R_0)}{\gamma_b^2 R_0} \left\{-\chi_{n,n}^{(0)}\hat{\phi}_n\right.$$

$$\left. + \Lambda\alpha\left[\chi_{n,n-1}^{(1)}\hat{A}_{n-1} + \chi_{n,n+1}^{(1)}\hat{A}_{n+1}\right]\right\} , \tag{54}$$

$$\left\{\frac{1}{r}\frac{\partial}{\partial r} r \frac{\partial}{\partial r} - \frac{1}{r^2} + \frac{\omega^2}{c^2} - (k + nk_0 + k_0)^2\right\} \hat{A}_{n+1}(r) = - \frac{\delta(r - R_0)}{R_0} \Lambda$$

$$\cdot \left\{\chi_{n,n}^{(1)}\hat{\phi}_n - \Lambda\alpha\left(\chi_{n,n-1}^{(2)}\hat{A}_{n-1} + \chi_{n,n+1}^{(2)}\hat{A}_{n+1}\right)\right\} , \tag{55}$$

$$\left\{\frac{1}{r}\frac{\partial}{\partial r} r \frac{\partial}{\partial r} - \frac{1}{r^2} + \frac{\omega^2}{c^2} - (k + nk_0 - k_0)^2\right\}\hat{A}_{n-1}(r) = - \frac{\delta(r - R_0)}{R_0} \Lambda$$

$$\cdot \left\{\chi_{n,n}^{(1)}\hat{\phi}_n - \Lambda\alpha\left(\chi_{n,n-1}^{(2)}\hat{A}_{n-1} + \chi_{n,n+1}^{(2)}\hat{A}_{n+1}\right)\right\} , \tag{56}$$

for a thin annular beam satisfying Eq. (1).

Since the right-hand side of Eq. (54) vanishes except at $r = R_0$, Eq. (54) can be expressed as

$$\left(\frac{1}{r}\frac{\partial}{\partial r} r \frac{\partial}{\partial r} + p_n^2\right)\hat{\phi}_n(r) = 0 , \tag{57}$$

for $r \neq R_0$. In Eq. (57), the parameter p_n^2 is defined by

$$p_n^2 = \omega^2/c^2 - (k + nk_0)^2 . \tag{58}$$

The solution to Eq. (54) is given by

$$\hat{\phi}_n(r) = \begin{cases} AJ_0(p_n r) + BN_0(p_n r) , & R_0 < r \leq R_c , \\ cJ_0(p_n r) , & 0 \leq r < R_0 , \end{cases} \tag{59}$$

where $J_\ell(x)$ and $N_\ell(x)$ are Bessel functions of the first and second

kind, respectively, of order ℓ, and R_c is the radius of the conducting wall (Fig. 1). In Eq. (59), the constants A, B, and C are determined by the boundary conditions that the effective potential $\hat{\phi}_n(r)$ vanishes at $r = R_c$, and that $\hat{\phi}_n(r)$ is continuous at $r = R_0$. Multiplying Eq. (54) by r and integrating from $R_0(1-\epsilon)$ to $R_0(1+\epsilon)$ with $\epsilon \to 0_+$, we obtain after some straightforward algebra,

$$\Gamma_{0,n}(\omega,k)\hat{\phi}_n(R_0) = \frac{\pi}{2\gamma_b^2} \{-\chi_{n,n}^{(0)}\hat{\phi}_n(R_0) + \Lambda\alpha[\chi_{n,n-1}^{(1)}\hat{A}_{n-1}(R_0) + \chi_{n,n+1}^{(1)}\hat{A}_{n+1}(R_0)]\},$$
(60)

where the dielectric function $\Gamma_{n',n}(\omega,k)$ is defined by

$$\Gamma_{n',n}(\omega,k) = \frac{J_{n'}(p_n R_c)/J_{n'}(p_n R_0)}{J_{n'}(p_n R_0)N_{n'}(p_n R_c) - J_{n'}(p_n R_c)N_{n'}(p_n R_0)}$$
(61)

and use has been made of the Wronskian identity,

$$J_{n'}(x)dN_{n'}(x)/dx - N_{n'}(x)dJ_{n'}(x)/dx = 2/\pi x .$$
(62)

Similarly, making use of Eqs. (55) and (56), we obtain

$$\Gamma_{1,n+1}(\omega,k)\hat{A}_{n+1}(R_0) = \frac{\pi}{2}\Lambda\{\chi_{n,n}^{(1)}\hat{\phi}_n(R_0) - \Lambda\alpha[\chi_{n,n-1}^{(2)}\hat{A}_{n-1}(R_0) + \chi_{n,n+1}^{(2)}\hat{A}_{n+1}(R_0)]\}$$
(63)

and

$$\Gamma_{1,n-1}(\omega,k)\hat{A}_{n-1}(R_0) = \frac{\pi}{2}\Lambda\{\chi_{n,n}^{(1)}\hat{\phi}_n(R_0) - \Lambda\alpha[\chi_{n,n-1}^{(2)}\hat{A}_{n-1}(R_0) + \chi_{n,n+1}^{(2)}\hat{A}_{n+1}(R_0)]\}.$$
(64)

In Eq. (63), $\Gamma_{1,n+1}$ is a function of $p_{n+1}^2 = \omega^2/c^2 - (k + nk_0 + k_0)^2$ defined in Eq. (58). From Eqs. (60), (63), and (64), we obtain the matrix equation relating $\hat{A}_{n+1}(R_0)$, $\hat{A}_{n-1}(R_0)$, and $\hat{\phi}_n(R_0)$

$$\begin{pmatrix} \Gamma_{1,n+1} + \frac{\pi}{2}\Lambda^2\alpha\chi_{n,n+1}^{(2)} , & \frac{\pi}{2}\Lambda^2\alpha\chi_{n,n-1}^{(2)} , & -\frac{\pi}{2}\Lambda\chi_{n,n}^{(1)} \\ \frac{\pi}{2}\Lambda^2\alpha\chi_{n,n+1}^{(2)} , & \Gamma_{1,n-1} + \frac{\pi}{2}\Lambda^2\alpha\chi_{n,n-1}^{(2)} , & -\frac{\pi}{2}\Lambda\chi_{n,n}^{(1)} \\ -\frac{\pi}{2\gamma_b^2}\Lambda\alpha\chi_{n,n+1}^{(1)}, & -\frac{\pi}{2\gamma_b^2}\Lambda\alpha\chi_{n,n-1}^{(1)}, & \Gamma_{0,n} + \frac{\pi}{2\gamma_b^2}\chi_{n,n}^{(0)} \end{pmatrix} \begin{pmatrix} \hat{A}_{n+1}(R_0) \\ \hat{A}_{n-1}(R_0) \\ \hat{\phi}_n(R_0) \end{pmatrix} = 0,$$
(65)

which is similar in general form to the matrix equation obtained by

Davidson et al.[1] for the free electron laser instability in a uniform

density electron beam. The dispersion relation can be obtained

from the condition that the determinant of the matrix in Eq. (65)

vanish.

Evidently, from Eq. (65), an explicit evaluation of the susceptibility $\chi_{n,n'}^{(j)}$, defined in Eq. (52) is required for a detailed stability analysis. Substituting Eqs. (22) and (42) into Eq. (52) gives

$$\chi_{n,n'}^{(j)} = 2\nu m c^2 \int_0^\infty dp_\perp^2 \int_{-\infty}^\infty dp_z \left\{ 2[\gamma m \omega - (k + n'k_0)p_z] \frac{\partial F}{\partial p_\perp^2} G \right.$$
$$\left. + (k + n'k_0)F \frac{\partial G}{\partial p_z} \right\} \frac{(\gamma_b/\gamma)^j}{[\omega - (k + nk_0)v_z]} \ , \tag{66}$$

where $\nu = N_b e^2/mc^2$ is Budker's parameter defined in Eq. (3), and use has been made of the identity

$$\int_0^{R_c} dr \ r \ \frac{\Theta[(r_2 - r)(r - r_1)]}{[(r_2^2 - r^2)(r^2 - r_1^2)]^{1/2}} = \frac{\pi}{2} \ .$$

In obtaining Eq. (66), the $p_\perp$ derivatives of $\Theta[(r_2 - r)(r - r_1)]$ $\times [(r^2 - r_1^2)(r_2^2 - r^2)]^{-1/2}$ and $\delta(\hat{\phi} - \hat{\phi}_0) + \delta(\hat{\phi} - \pi + \hat{\phi}_0)$ have

been neglected, since the corresponding corrections are of order $|\omega - (k + nk_0)V_b|/|\omega_c + k_0 V_b| \ll 1$, or smaller. Equation (66) can

be further simplified by integrating by parts and making use of

$$F(0) = F(\infty) = G(\infty) = G(-\infty) = 0 \ .$$

Within the context of Eqs. (3) and (14), we obtain

$$\chi_{n,n'}^{(j)} = \frac{2\nu}{\gamma_b} [\omega^2 - (k + nk_0)(k + n'k_0)c^2] \int_0^\infty dp_\perp^2 \int_{-\infty}^\infty dp_z \left(\frac{\gamma_b}{\gamma}\right)^{j+1}$$
$$\times \frac{F(p_\perp^2)G(p_z)}{[\omega - (k + nk_0)p_z/\gamma m]^2} \ , \tag{67}$$

after some straightforward algebra. Equations (65) and (67) describe
stability behavior for general choice of equilibrium distribution function
$F(p_\perp^2)G(p_z)$, and can be used to investigate stability properties for a
broad range of system parameters.

IV. STABILITY PROPERTIES

A. General Dispersion Relation

As an example, in this section we investigate free electron laser stability properties for an electron beam with perpendicular distribution function,

$$F(p_\perp^2) = \delta(p_\perp^2 - p_{\perp 0}^2), \tag{68}$$

where $p_{\perp 0}$ = const. is related to the radial thickness of the beam.[11] Moreover, in order to investigate the influence of axial momentum spread on the free electron laser instability, we assume an axial momentum distribution function of the form

$$G(p_z) = \frac{\Delta}{\pi} \frac{1}{(p_z - p_b)^2 + \Delta^2} , \tag{69}$$

where Δ is the characteristic momentum spread about the mean momentum $p_b = \gamma_b m V_b$. We further assume that the momentum spread Δ is small in comparison with the directed momentum p_b, i.e.,

$$\Delta \ll p_b. \tag{70}$$

For small values of $\delta p_z = p_z - p_b$ consistent with Eq. (70), we can approximate the term $p_z/\gamma m$ in Eq. (67) by

$$\frac{p_z}{\gamma m} = \frac{p_b}{\gamma_b m} + \frac{\delta p_z}{\gamma_b^3 m} , \tag{71}$$

where $\gamma_b = (1 + p_b^2/m^2 c^2)^{1/2}$.

Substituting Eqs. (68) - (71) into Eq. (67), we obtain

$$\chi_{n,n'}^{(j)} = \chi_{n,n'}^{(0)} = \frac{2\nu}{\gamma_b} \frac{[\omega^2 - (k + nk_0)(k + n'k_0)c^2]}{[\omega - (k + nk_0)V_b + i|k + nk_0|\Delta/\gamma_b^3 m]^2} , \tag{72}$$

within the context of Eq. (14). Equation (65) can be simplified

considerably by making use of Eq. (72). The condition for a non-

trivial solution to Eq. (65) is that the determinant of the

matrix vanish. This gives the general dispersion relation

$$\Gamma_{1,n+1}\Gamma_{1,n-1}\left(\Gamma_{0,n} + \frac{\pi}{2\gamma_b^2}\chi_{n,n}^{(0)}\right)$$

$$= -\frac{\pi}{2}\alpha\Lambda^2[\Gamma_{1,n+1}\chi_{n,n-1}^{(0)} + \Gamma_{1,n-1}\chi_{n,n+1}^{(0)}]\Gamma_{0,n} , \tag{73}$$

which can be used to determine the complex eigenfrequency ω in terms of

$k + nk_0$, k_0, ν, Δ, and Λ. What is most remarkable is that Eq. (73)

is very similar in general form to the result obtained by Davidson et al.[1]

for a uniform density electron beam.

Consistent with Eqs. (3) and (14), the eigenfrequency ω can be

approximated by $\omega \simeq (k + nk_0)V_b$. We therefore approximate p_n and

p_{n+1} in Eq. (58) by

$$p_n = iq_n = i(k + nk_0)/\gamma_b , \tag{74}$$

and

$$p_{n+1} = iq_{n+1} = i[q_n^2 + 2k_0(k + nk_0) + k_0^2]^{1/2} . \tag{75}$$

Making use of Eqs. (74) and (75), the dielectric functions $\Gamma_{1,n+1}$

and $\Gamma_{0,n}$ can be expressed as

$$\Gamma_{1,n+1} = \frac{\pi}{2}\frac{I_1(q_{n+1}R_c)/I_1(q_{n+1}R_0)}{I_1(q_{n+1}R_c)K_1(q_{n+1}R_0) - I_1(q_{n+1}R_0)K_1(q_{n+1}R_c)} \tag{76}$$

and

$$\Gamma_{0,n} = \frac{\pi}{2}h(q_nR_0) \equiv \frac{\pi}{2}\frac{I_0(q_nR_c)/I_0(q_nR_0)}{I_0(q_nR_c)K_0(q_nR_0) - I_0(q_nR_0)K_0(q_nR_c)} , \tag{77}$$

for $k + nk_0 \geq 0$. In Eqs. (76) and (77), $I_\ell(x)$ and $K_\ell(x)$ are modified

Bessel functions of the first and second kind, respectively, of order ℓ,

and $h(q_n R_0)$ is the effective electrostatic wave admittance. Note from Eqs. (76) and (77) that the dielectric functions $\Gamma_{0,n}$ and $\Gamma_{1,n+1}$ are generally nonzero monotonic increasing functions of $q_n R_0$ and $q_{n+1} R_0$, respectively. In this regard, for small wiggler amplitude ($\Lambda \ll 1$), we investigate free electron laser stability properties for ω and $k + n k_0$ near the simultaneous zeroes of the transverse dispersion relation $\Gamma_{1,n-1} = 0$, and the longitudinal dispersion relation $\Gamma_{0,n} + (\pi/2\gamma_b^2)\chi_{n,n}^{(0)} = 0$. The general dispersion relation in Eq. (73) can then be approximated by the simplified form

$$\Gamma_{1,n-1}\left(\Gamma_{0,n} + \frac{\pi}{2\gamma_b^2}\chi_{n,n}^{(0)}\right) = -\frac{\pi}{2}\,\alpha\Lambda^2\chi_{n,n-1}^{(0)}\Gamma_{0,n} \;. \tag{78}$$

Equation (78) is the form of the dispersion relation used in the remainder of Sec. IV.

B. Linear Eigenmode Properties

For very small wiggler amplitude ($\Lambda \to 0$), or for very low beam density ($\nu \to 0$), it is evident from Eq. (78) that the linear dispersion relation for transverse electromagnetic perturbations is given by

$$\Gamma_{1,n-1}(\omega,k) = 0 \;, \tag{79}$$

and the linear dispersion relation for longitudinal perturbations is given by

$$\Gamma_{0,n}(\omega,k) + \frac{\pi}{2\gamma_b^2}\chi_{n,n}^{(0)} = 0 \;. \tag{80}$$

Here, we assume $k + n k_0 \geq 0$, and the eigenfrequency ω satisfies $\omega \simeq (k + n k_0) V_b$ for a low-density beam. Equation (79) can be expressed in the equivalent form

$$\frac{\omega^2}{c^2} - (k + nk_0 - k_0)^2 = \frac{\alpha_{0s}^2}{R_c^2} , \tag{81}$$

where α_{0s} is the s'th root of $J_1(\alpha_{0s}) = 0$, and use has been made of the definition in Eq. (61). Equation (81) is the familiar vacuum waveguide electromagnetic dispersion relation. For future reference, Taylor expanding the electromagnetic dielectric function $\Gamma_{1,n-1}$ in Eq. (61) about $[\omega^2/c^2 - (k + nk_0 - k_0)^2]R_c^2 = \alpha_{0s}^2$, it is straight-forward to show that $\Gamma_{1,n-1}$ can be approximated by

$$\Gamma_{1,n-1}(\omega,k) = - \frac{\pi R_c^2}{4} \left(\frac{\omega^2}{c^2} - (k + nk_0 - k_0)^2 - \frac{\alpha_{0s}^2}{R_c^2} \right) \left(\frac{J_2(\alpha_{0s})}{J_1(\alpha_{0s}R_0/R_c)} \right)^2 . \tag{82}$$

Moreover, making use of Eqs. (72) and (77), it can also be shown that the effective longitudinal dielectric function is given by

$$1 + \frac{\pi}{2\gamma_b^2} \frac{\chi_{n,n}^{(0)}}{\Gamma_{0,n}} \tag{83}$$

$$= 1 - \frac{2\nu}{\gamma_b^3 h} \frac{[(k + nk_0)^2 c^2 - \omega^2]}{[\omega - (k + nk_0)V_b + i|k + nk_0|\Delta/\gamma_b^3 m]^2} .$$

The expression for the electrostatic wave admittance $h(q_n R_0)$ in Eq. (77) can be simplified in several limiting cases. These include:

(a) Long wavelength perturbations with $q^2 R_0^2 \ll 1$. In this case, $h(q_n R_0)$ can be approximated by

$$h(q_n R_0) = [\ln(R_c/R_0)]^{-1} .$$

(b) Large conducting wall radius (i.e., $R_c/R_0 \to \infty$). In this case

$$h(q_n R_0) = [I_0(q_n R_0) K_0(q_n R_0)]^{-1} .$$

(c) Short wavelength perturbations with $q_n^2 R_0^2 \gg 1$. In this case, $h(q_n R_0)$ can be approximated by

$$h(q_n R_0) = q_n R_0 [1 + \coth q_n (R_c - R_0)] .$$

It is instructive to examine the longitudinal linear dispersion relation in Eq. (80) for perturbations with long axial wavelength and $\Delta \to 0$. Keep in mind that $\Delta \to 0$ corresponds to a cold axial distribution function $G(p_z) = \delta(p_z - p_b)$. Making use of Eq. (83) in the cold-beam limit, we find that Eq. (80) can be approximated by

$$[\omega - (k + nk_0)V_b]^2 = \frac{2\nu}{\gamma_b^3} [(k + nk_0)^2 c^2 - \omega^2] \ell n(R_c/R_0) , \qquad (84)$$

which is identical to the dispersion relation obtained by Briggs[12] for space-charge waves in a thin annular electron beam.

To further orient the reader and illustrate the interaction wavenumbers and frequencies characteristic of the free electron laser instability, we consider a tenuous electron beam with $\nu \to 0$ and $\Delta \to 0$, and determine the simultaneous solutions to Eqs. (79) and (80). Evidently, making use of Eq. (83), the longitudinal dispersion relation in Eq. (80) reduces to

$$\omega = (k + nk_0)V_b , \qquad (85)$$

for $\nu \to 0$ and $\Delta \to 0$. Solving Eqs. (81) and (85) simultaneously, we obtain the interaction frequency

$$\omega = \omega^\pm = \gamma_b^2 k_0 V_b \{1 \pm [1 - (1 - \alpha_{0s}^2/k_0^2 R_c^2)/\gamma_b^2]^{1/2}\} , \qquad (86)$$

where ω^+ and ω^- represent the upshifted and downshifted frequencies, respectively. In the limit of short wiggler wavelength satisfying

$k_0^2 R_c^2 \gg \alpha_{0s}^2$, the upshifted frequency ω^+ and wavenumber $(k + nk_0)^+$ can be approximated by the familiar results

$$\omega^+ = (1 + \beta_b)\gamma_b^2 k_0 V_b , \qquad (87)$$

$$(k + nk_0)^+ = (1 + \beta_b)\gamma_b^2 k_0 ,$$

obtained in free electron laser theories neglecting geometric effects. For sufficiently long wiggler wavelength, however, it is evident from Eq. (86) that geometric effects play a significant role in determining the characteristic frequency and wavenumber.

Finally, for small but finite wiggler amplitude and beam density, we make use of Eqs. (72), (82), and (83), to simplify the full dispersion relation in Eq. (78). This gives

$$\left\{\frac{\omega^2}{c^2} - (k + nk_0 - k_0)^2 - \frac{\alpha_{0s}^2}{R_c^2}\right\} \left\{\left(\omega - (k + nk_0)V_b + i\frac{|k + nk_0|\Delta}{\gamma_b^3 m}\right)^2\right.$$

$$\left. - \frac{2\nu c^2}{\gamma_b^3 h}\left[2k_0(k + nk_0) - k_0^2 - \frac{\alpha_{0s}^2}{R_c^2}\right]\right\} \qquad (88)$$

$$= -4\alpha\Lambda^2 \frac{\nu c^2}{\gamma_b}\left[k_0(k + nk_0 - k_0) - \frac{\alpha_{0s}^2}{R_c^2}\right]\left[\frac{J_1(\alpha_{0s}R_0/R_c)}{R_c^2 J_2(\alpha_{0s})}\right]^2 ,$$

where use has been made of Eq. (81) to simplify the right-hand side of Eq. (88). Equation (88) is the form of the nonlinear dispersion relation used in the numerical studies in Sec. IV.C.

C. Numerical Analysis of the Dispersion Relation

In this section, we summarize the results of a numerical analysis of the dispersion relation in Eq. (88) for a broad range of system parameters ν, γ_b, $\Delta/\gamma_b mc$, $\alpha_{0s}/k_0 R_c$ and

$$\varepsilon = \alpha\left(\frac{e\beta}{\gamma_b mk_0 c^2}\right)^2 . \qquad (89)$$

Defining the normalized Doppler-shifted eigenfrequency by

$$\Omega = [\omega - (k + nk_0)V_b]/k_0 c , \tag{90}$$

the dispersion relation in Eq. (85) can be expressed as

$$\left(\Omega^2 + 2\frac{(k + nk_0)V_b}{k_0 c}\Omega + \xi\right)\left(\Omega^2 + 2i\frac{(k + nk_0)\Delta}{\gamma_b^3 m k_0 c}\Omega - \eta\right) + \zeta = 0 , \tag{91}$$

where

$$\xi = 2(k + nk_0)/k_0 - (k + nk_0)^2/k_0^2\gamma_b^2 - 1 - \alpha_{0s}^2/k_0^2 R_c^2 , \tag{92}$$

$$\eta = (k + nk_0)^2\Delta^2/\gamma_b^6 m^2 k_0^2 c^2 + (2\nu/\gamma_b^3 h)[2(k + nk_0)/k_0 - \alpha_{0s}^2/k_0^2 R_c^2 - 1] , \tag{93}$$

and

$$\zeta = \frac{\epsilon}{4}\frac{\nu}{\gamma_b}\left(\frac{k + nk_0}{k_0} - 1 - \frac{\alpha_{0s}^2}{k_0^2 R_c^2}\right)\left[\left(\frac{R_0}{R_c}\right)\frac{J_1(\alpha_{0s}R_0/R_c)}{J_2(\alpha_{0s})}\right]^2 . \tag{94}$$

A careful examination of Eqs. (91) and (94) shows that the maximum coupling between the electromagnetic and electrostatic modes occurs at the value of R_0/R_c satisfying

$$J_1(\alpha_{0s}R_0/R_c) + (\alpha_{0s}R_0/R_c)J_1'(\alpha_{0s}R_0/R_c) = 0 , \tag{95}$$

where the prime (') denotes $dJ_1(x)/dx$. Making use of the identity $J_1'(x) = J_0(x) - J_1(x)/x$, Eq. (95) can be expressed in the equivalent form

$$J_0(\alpha_{0s}R_0/R_c) = 0 . \tag{96}$$

In this context, we find that the maximum growth rate occurs for the value of R_0/R_c given by

$$R_0/R_c = \beta_{0\ell}/\alpha_{0s} , \tag{97}$$

where $\beta_{0\ell}$ is the ℓth root of $J_0(\beta_{0\ell}) = 0$ satisfying $\beta_{0\ell} < \alpha_{0s}$.

Figure 2 shows a plot of the electrostatic wave admittance h versus normalized axial wavenumber $(k + nk_0)/k_0$ for $\gamma_b = 5$, $k_0 R_c = 5$, and $R_0/R_c = \beta_{01}/\alpha_{01} = 0.65$. We note from Fig. 2 that the wave admittance h is proportional to the axial wavenumber $(k + nk_0)$ for wavenumbers satisfying $(k + nk_0)/k_0 > 5$. For short axial wavelengths with $(R_c - R_0) \times (k + nk_0) \gg \gamma_b$, it is readily shown from Eq. (77) that the wave admittance h can be approximated by

$$h = \left(2 \, \frac{k_0 R_c}{\gamma_b} \, \frac{R_0}{R_c} \right) \frac{k + nk_0}{k_0} \, . \tag{98}$$

For free electron laser applications characterized by axial wavenumber $k + nk_0 \simeq (1 + \beta_b)\gamma_b^2 k_0$, Eq. (98) constitutes an excellent approximation.

Shown in Fig. 3 for $\epsilon = -0.1$, and in Fig. 4 for $\epsilon = +0.1$, are plots of (a) normalized growth rate $\Omega_i = \text{Im}\Omega$ and (b) Doppler-shifted real frequency $\Omega_r = \text{Re}\Omega$ versus the normalized axial wavenumber $(k + nk_0)/k_0$, obtained from Eq. (91) for $\Delta = 0$ and parameters otherwise identical to Fig. 2. In Figs. 3(b) and 4(b), Ω_r is plotted only for the range of wavenumber $(k + nk_0)/k_0$ corresponding to instability $(\Omega_i > 0)$. Evidently, from Figs. 3(a) and 4(a), the maximum growth rate and the range of $(k + nk_0)$ corresponding to instability, increase with increasing value of beam intensity. It is also evident from Figs. 3(a) and 4(a) that the instability occurs at values of axial wavenumber satisfying $(k + nk_0)/k_0 < 2\gamma_b^2$ for $\epsilon < 0$, and $(k + nk_0)/k_0 > 2\gamma_b^2$ for $\epsilon > 0$. Moreover, the normalized Doppler-shifted eigenfrequency satisfies $|\Omega| \ll 1$, which is consistent with Eq. (14).

The dependence of stability properties on the axial momentum spread (Δ) is illustrated in Fig. 5(a) for $\epsilon = -0.1$, and in Fig. 5(b) for $\epsilon = +0.1$, where the normalized growth rate Ω_i is plotted versus $(k + nk_0)/k_0$ for $\nu/\gamma_b = 0.05$, several values of $\Delta/\gamma_b mc$, and parameters

otherwise identical to Fig. 2. Several features are noteworthy from
Fig. 5. First, the maximum growth rate decreases as the axial momentum
spread is increased. Evidently, the growth rate is reduced substantially
by introducing a very small amount of momentum spread. From Eq. (91),
this feature represents a general tendency for all radial mode numbers s.
Second, the instability bandwidth, i.e., the range of $(k + nk_0)/k_0$
corresponding to instability, increases as $\Delta/\gamma_b mc$ is increased. Third,
for a specified value of ϵ, the maximum growth rate occurs at approximately
the same value of axial wavenumber, regardless of the momentum spread
(e.g., at $k + nk_0 = 45.3 \ k_0$ for $\epsilon = -0.1$, and at $k + nk_0 = 53 \ k_0$ for
$\epsilon = 0.1$). Finally, we also note that a sign change of the parameter ϵ
shifts the unstable region in $(k + nk_0)$ space. Moreover, for a given
value of Δ, the maximum growth rate for $\epsilon = -0.1$ is slightly larger
than that for $\epsilon = 0.1$. In general, we conclude that free electron
laser stability properties exhibit a sensitive dependence on the axial
momentum spread Δ.

V. CONCLUSIONS

In this paper, we have formulated a self-consistent theory
of the free electron laser instability for an annular beam propagating
through an undulator magnetic field. The stability analysis has been
carried out within the framework of the Vlasov-Maxwell equations. The
equilibrium properties and basic assumptions were summarized in Sec. II,
and the formal stability analysis for azimuthally symmetric perturbations
($\partial/\partial \theta = 0$) was carried out in Sec. III, including the important influence
of finite radial geometry. In Sec. IV, the dispersion relation
was obtained for perturbations about an annular beam equilibrium
in which all electrons have the same value of transverse momentum
and the same value of canonical angular momentum, and a Lorentzian
distribution in axial momentum. One of the most important features of
the analysis is that the maximum growth rate occurs for $R_0/R_c = \beta_{0\ell}/\alpha_{0s}$.
Moreover, the growth rate and instability bandwidth can be expressed in
terms of Budker's parameter ν, instead of the beam plasma frequency
as in the case of a uniform density beam. In Sec. IV, it was
shown that stability properties exhibit a sensitive dependence on axial
momentum spread Δ.

ACKNOWLEDGMENTS

REFERENCES

1. R. C. Davidson and H. S. Uhm, Phys. Fluids 23, in press (1980).

2. H. Motz, J. Appl. Phys. 22, 527 (1950).

3. T. Kwan and J. M. Dawson, Phys. Fluids 22, 1089 (1979).

4. P. Sprangle and R. A. Smith, Phys. Rev. A21, 293 (1980).

5. A. T. Lin and J. M. Dawson, Phys. Fluids 23, 1224 (1980).

6. P. Sprangle, C. M. Tang, and W. M. Manheimer, Phys. Rev. A21, 302 (1980).

7. I. B. Bernstein and J. L. Hirshfield, Phys. Rev. A20, 1661 (1979).

8. T. C. Marshall, S. Talmadge, and P. Efthimion, Appl. Phys. Lett. 31, 320 (1977).

9. D. A. G. Deacon, L. R. Elias, J. M. M. Madey, G. J. Ramian, H. A. Schwettman, and T. I. Smith, Phys. Rev. Lett. 38, 897 (1977).

10. L. R. Elias, W. M. Fairbank, J. M. J. Madey, H. A. Schwettman, and T. I. Smith, Phys. Rev. Lett. 36, 717 (1976).

11. H. S. Uhm and R. C. Davidson, Phys. Fluids 22, 1811 (1979).

12. R. J. Briggs, Phys. Fluids 19, 1257 (1976).

FIGURE CAPTIONS

Fig. 1 Equilibrium configuration and coordinate system.

Fig. 2 Plot of electrostatic wave admittance h versus $(k + nk_0)/k_0$

for $\gamma_b = 5$, $k_0 R_c = 5$, and $R_0/R_c = \beta_{01}/\alpha_{01} = 0.65$.

Fig. 3 Plots of (a) normalized growth rate Ω_i and (b) Doppler-shifted

real frequency Ω_r versus $(k + nk_0)/k_0$ [Eq. (91)] for $\epsilon = -0.1$,

$\Delta = 0$ and parameters otherwise identical to Fig. 2.

Fig. 4 Plots of (a) normalized growth rate Ω_i and (b) Doppler-shifted

real frequency Ω_r versus $(k + nk_0)/k_0$ [Eq. (91)] for $\epsilon = 0.1$,

$\Delta = 0$, and parameters otherwise identical to Fig. 2.

Fig. 5 Plots of normalized growth rate Ω_i versus $(k + nk_0)/k_0$ [Eq. (91)]

for $\nu/\gamma_b = 0.05$, (a) $\epsilon = -0.1$, (b) $\epsilon = 0.1$, several values of

$\Delta/\gamma_b mc$, and parameters otherwise identical to Fig. 2.

APPENDIX A

ELECTRON TRAJECTORIES IN AN UNDULATOR MAGNETIC FIELD

In this appendix, we determine the particle trajectories $(r', \theta', z', p_r', p_\theta', p_z')$ that pass through the phase-space point $(r, \theta, z, p_r, p_\theta, p_z)$ at time $t' = t$ for an electron moving in the undulator wiggler field described by [Eqs. (8) and (9)],

$$B_r^0 = -\frac{1}{2} \hat{B} k_0 R_0 \sin k_0 z, \tag{A.1}$$

$$B_z^0 = B_0 - \hat{B}_z \cos k_0 z, \tag{A.2}$$

where $\lambda_0 = 2\pi/k_0$ is the wiggler wavelength, $\hat{B}_z = \text{const.}$ is the amplitude, and $B_0 = \text{const.}$ is the average axial magnetic field. Making use of $P_\theta = P_0 = -eB_0 R_0^2/2c = \text{const.}$, and $\gamma mc^2 = (m^2 c^4 + c^2 \underset{\sim}{p}'^2)^{1/2} = \text{const.}$, the exact equations of motion can be expressed as

$$\frac{d^2}{dt'^2} r' - r'\left(\frac{d\theta'}{dt'}\right)^2 = r'\left(\frac{d\theta'}{dt'}\right) \frac{eB_0}{\gamma mc}\left[1 - \frac{\hat{B}_z}{B_0} \cos k_0 z'\right], \tag{A.3}$$

$$r'\frac{d\theta'}{dt'} = -\frac{eB_0}{2\gamma mc}\left[\frac{R_0^2}{r'} - r'\left(1 - \frac{\hat{B}}{B_0}\frac{R_0}{r'}\frac{I_1(k_0 r')}{I_1(k_0 R_0)} \cos k_0 z'\right)\right], \tag{A.4}$$

$$\frac{d^2 z'}{dt'^2} = -\frac{eB_0}{2\gamma mc} k_0 R_0 \left(r'\frac{d\theta'}{dt'}\right) \frac{\hat{B}}{B_0} \sin k_0 z', \tag{A.5}$$

where $v_r' = p_r'/\gamma m = dr'/dt'$, $v_\theta' = p_\theta'/\gamma m = r'd\theta'/dt'$, $v_z' = p_z'/\gamma m = dz'/dt'$, and use has been made of the expression for $A_\theta^0(r', z')$ in Eq. (7).

We now examine solutions to Eqs. (A.3) – (A.5) that pass through the phase space point $(r, \theta, z, p_r, p_\theta, p_z)$ at time $t' = t$, assuming that the wiggler amplitude is small with

$$\frac{\hat{B}_z}{B_0} = \frac{1}{2} k_0 R_0 \frac{I_0(k_0 R_0)}{I_1(k_0 R_0)} \frac{\hat{B}}{B_0} \ll 1. \qquad (A.6)$$

Moreover, in the subsequent analysis we denote the small radial excursions about $r' = R_0$ by the radial coordinate

$$\rho' = r' - R_0. \qquad (A.7)$$

To lowest order in $\hat{B}/B_0$, we find from Eq. (A.5) that the axial motion is free streaming with

$$z' = z + \frac{p_z}{\gamma m} (t' - t), \qquad (A.8)$$

$$p_z' = p_z. \qquad (A.9)$$

Substituting Eq. (A.4) into Eq. (A.3) and making use of Eq. (A.7), the radial equation of motion can be expressed as

$$\frac{d^2 \rho'}{dt'^2} = \left(\frac{eB_0}{2\gamma mc} \right)^2 \left[\frac{R_0^2}{R_0 + \rho'} - (R_0 + \rho') + \frac{\hat{B}}{B_0} R_0 \frac{I_1(k_0 R_0 + k_0 \rho')}{I_0(k_0 R_0)} \cos k_0 z' \right]$$

$$\times \left[\frac{R_0^2}{(R_0 + \rho')^2} + 1 + \frac{\hat{B}}{B_0} \frac{R_0}{R_0 + \rho'} \frac{I_1(k_0 R_0 + k_0 \rho')}{I_1(k_0 R_0)} \cos k_0 z' \right. \qquad (A.10)$$

$$\left. - \frac{\hat{B}}{B_0} k_0 R_0 \frac{I_0(k_0 R_0)}{I_1(k_0 R_0)} \cos k_0 z' \right] .$$

Expanding the right-hand side of Eq. (A.10) for $\hat{B} \ll B_0$ and $|\rho'| \ll R_0$, and making use of Eq. (A.8), we find to lowest order

$$\frac{d^2\rho'}{dt'^2} + \omega_c^2\rho' = \frac{1}{2}\omega_c^2 R_0 \frac{\hat{B}}{B_0} \cos\left[k_0 z + k_0 \frac{p_z}{\gamma m}(t' - t)\right] , \qquad (A.11)$$

where $\omega_c = eB_0/\gamma mc$ is the relativistic cyclotron frequency. The radial motion determined from Eq. (A.11) exhibits a strong resonance whenever $k_0 v_z = \omega_c$, where $v_z = p_z/\gamma m$ is the axial velocity. In the present analysis, we assume that the values of k_0, ω_c, and the characteristic axial velocity are such that resonance does not occur, i.e.,

$$k_0^2 v_z^2 \neq \omega_c^2 . \qquad (A.12)$$

Integrating Eq. (A.11) subject to the boundary conditions $(\rho', p_r') = (\rho, p_r)$ at time $t' = t$, the radial motion is described by

$$\rho' = \rho\cos\omega_c\tau + \frac{p_r}{\gamma m\omega_c}\sin\omega_c\tau$$

$$+ \frac{1}{2}R_0 \frac{\hat{B}}{B_0} \frac{\omega_c^2}{\omega_c^2 - k_0^2 v_z^2}\left[\cos(k_0 z + k_0 v_z\tau)\right. \qquad (A.13)$$

$$\left. - \left(\cos k_0 z\cos\omega_c\tau + \frac{k_0 v_z}{\omega_c}\sin k_0 z\sin\omega_c\tau\right)\right] ,$$

$$p_r' = p_r\cos\omega_c\tau - \gamma m\omega_c\rho\sin\omega_c\tau$$

$$+ \frac{1}{2}\gamma m R_0 \frac{\hat{B}}{B_0} \frac{\omega_c^2}{\omega_c^2 - k_0^2 v_z^2}[-k_0 v_z\sin(k_0 z + k_0 v_z\tau) \qquad (A.14)$$

$$+ (\omega_c\cos k_0 z\sin\omega_c\tau - k_0 v_z\sin k_0 z\cos\omega_c\tau)] ,$$

where $v_z = p_z/\gamma m$ and $\tau = t' - t$. Note from Eq. (A.13) that the radial excursions about $r = R_0$ remain small amplitude as long as

$$\left| \frac{\hat{B}}{B_0} \frac{\omega_c^2}{\omega_c^2 - k_0^2 v_z^2} \right| \lesssim \frac{2a}{R_0} , \qquad (A.15)$$

where 2a is the characteristic radial thickness of the annular electron beam. Finally, for the θ'-motion, we expand Eq. (A.4) for $\hat{B} \ll B_0$ and $|\rho'| \ll R_0$. To lowest order, this gives

$$\frac{d\theta'}{dt'} = \omega_c \frac{\rho'}{R_0} - \frac{1}{2} \omega_c \frac{\hat{B}}{B_0} \cos k_0 z' . \qquad (A.16)$$

Substituting Eq. (A.13) into Eq. (A.16), we obtain

$$\frac{d\theta'}{dt'} = \frac{\rho}{R_0} \omega_c \cos\omega_c\tau + \frac{P_r}{\gamma m R_0} \sin\omega_c\tau$$

$$- \frac{1}{2} \frac{\hat{B}}{B_0} \frac{\omega_c^2}{\omega_c^2 - k_0^2 v_z^2} \left(\omega_c \cos k_0 z \cos\omega_c\tau \right. \qquad (A.17)$$

$$\left. + k_0 v_z \sin k_0 z \sin\omega_c\tau - \frac{k_0^2 v_z^2}{\omega_c} \cos(k_0 z + k_0 v_z \tau) \right) .$$

In addition, the azimuthal momentum is readily determined from $p_\theta' = \gamma m r' d\theta'/dt' \simeq \gamma m \omega_c \rho' - (\gamma m \omega_c R_0/2)(\hat{B}/B_0)\cos k_0 z'$, where ρ' and z' are defined in Eqs. (A.13) and (A.8), respectively.

We conclude this appendix by noting that Eq. (A.5) can be used to calculate corrections to the lowest-order z-motion in Eqs. (A.8) and (A.9). Expanding the right-hand side of Eq. (A.5) for $|\rho'| \ll R_0$ and $\hat{B} \ll B_0$, and making use of Eq. (A.16) gives

$$\frac{d}{dt'} p_z' = - \frac{1}{2} \omega_c (k_0 R_0)(\gamma m \omega_c R_0) \frac{\hat{B}}{B_0}$$

$$\qquad\qquad (A.18)$$

$$\times \left(\frac{\rho'}{R_0} - \frac{1}{2} \frac{\hat{B}}{B_0} \cos k_0 z' \right) \sin k_0 z' ,$$

where $p_z' = \gamma m dz'/dt'$. Substituting the expressions for z' [Eq. (A.8)] and ρ' [Eq. (A.13)] into the right-hand side of Eq. (A.18) and integrating with respect to t', we find

$$
\begin{aligned}
p_z' = p_z &+ \frac{1}{2}\,\omega_c(k_0 R_0)(\gamma m \omega_c R_0)\,\frac{\hat{B}}{B_0} \\
&\times \left\{\left(\frac{\rho}{R_0} - \frac{1}{2}\frac{\hat{B}}{B_0}\frac{\omega_c^2}{\omega_c^2 - k_0^2 v_z^2}\cos k_0 z\right)\frac{1}{\omega_c^2 - k_0^2 v_z^2}\right. \\
&\qquad \times \left[\omega_c\Big(\cos(k_0 z + k_0 v_z \tau)\cos\omega_c\tau - \cos k_0 z\Big)\right. \\
&\qquad\qquad \left. + k_0 v_z \sin(k_0 z + k_0 v_z \tau)\sin\omega_c\tau\right] \\
&\quad + \left(\frac{p_r}{\gamma m \omega_c R_0} - \frac{1}{2}\frac{\hat{B}}{B_0}\frac{\omega_c k_0 v_z}{\omega_c^2 - k_0^2 v_z^2}\sin k_0 z\right)\frac{1}{\omega_c^2 - k_0^2 v_z^2} \\
&\qquad \times \left[\omega_c\Big(\sin(k_0 z + k_0 v_z \tau)\cos\omega_c\tau - \sin k_0 z\Big)\right. \\
&\qquad\qquad \left. - k_0 v_z \cos(k_0 z + k_0 v_z \tau)\sin\omega_c\tau\right] \\
&\quad \left. + \frac{1}{8}\frac{\hat{B}}{B_0}\frac{k_0 v_z}{\omega_c^2 - k_0^2 v_z^2}[\cos(2k_0 z + 2k_0 v_z \tau) - \cos 2k_0 z]\right\},
\end{aligned}
$$

(A.19)

where $\tau = t' - t$, $v_z = p_z/\gamma m$, and $p_z' = p_z$ at time $t' = t$.
Note from Eq. (A.19) that the oscillatory corrections to $p_z' = p_z$
[Eq. (A.9)] are small whenever the wiggler amplitude $\hat{B}$ is sufficiently small in comparison with B_0. Expressing Eq. (A.19) as $p_z' = p_z + \delta p_z'$, the inequality $|\delta p_z'| \ll |p_z|$ is hardest to satisfy in the strong magnetic field limit where $\omega_c^2 \gg k_0^2 v_z^2$. For $\omega_c^2 \gg k_0^2 v_z^2$, we find from Eq. (A.19) that $|\delta p_z'| \ll |p_z|$ provided the inequalities

$$\frac{1}{2} \frac{a}{R_0} \frac{\hat{B}}{B_0} (k_0 R_0) \left(\frac{\omega_c R_0}{v_z} \right) \ll 1 , \tag{A.20}$$

and

$$\frac{1}{4} \frac{\hat{B}^2}{B_0^2} (k_0 R_0) \left(\frac{\omega_c R_0}{v_z} \right) \ll 1 , \tag{A.21}$$

are satisfied. In obtaining Eq. (A.20), we have estimated the characteristic value of ρ by $\rho \approx a$, where $2a$ is the thickness of the annular electron beam. The inequalities in Eqs. (A.20) and (A.21) are straightforward to satisfy for experimental parameters of interest. Note also that $p_z' \simeq p_z$ whenever Eqs. (A.20) and (A.21) are satisfied, and the axial momentum p_z is a good (albeit approximate) invariant.
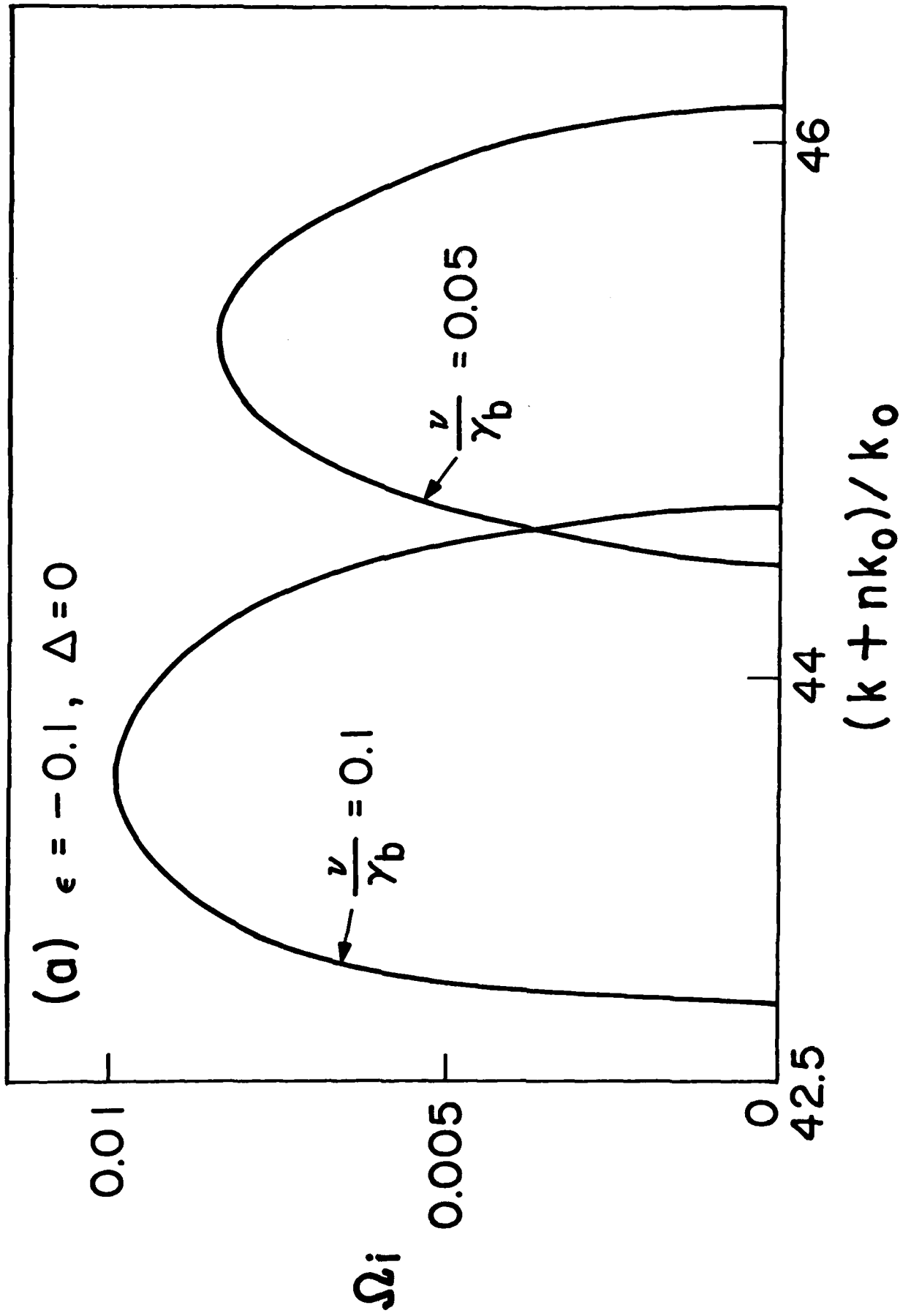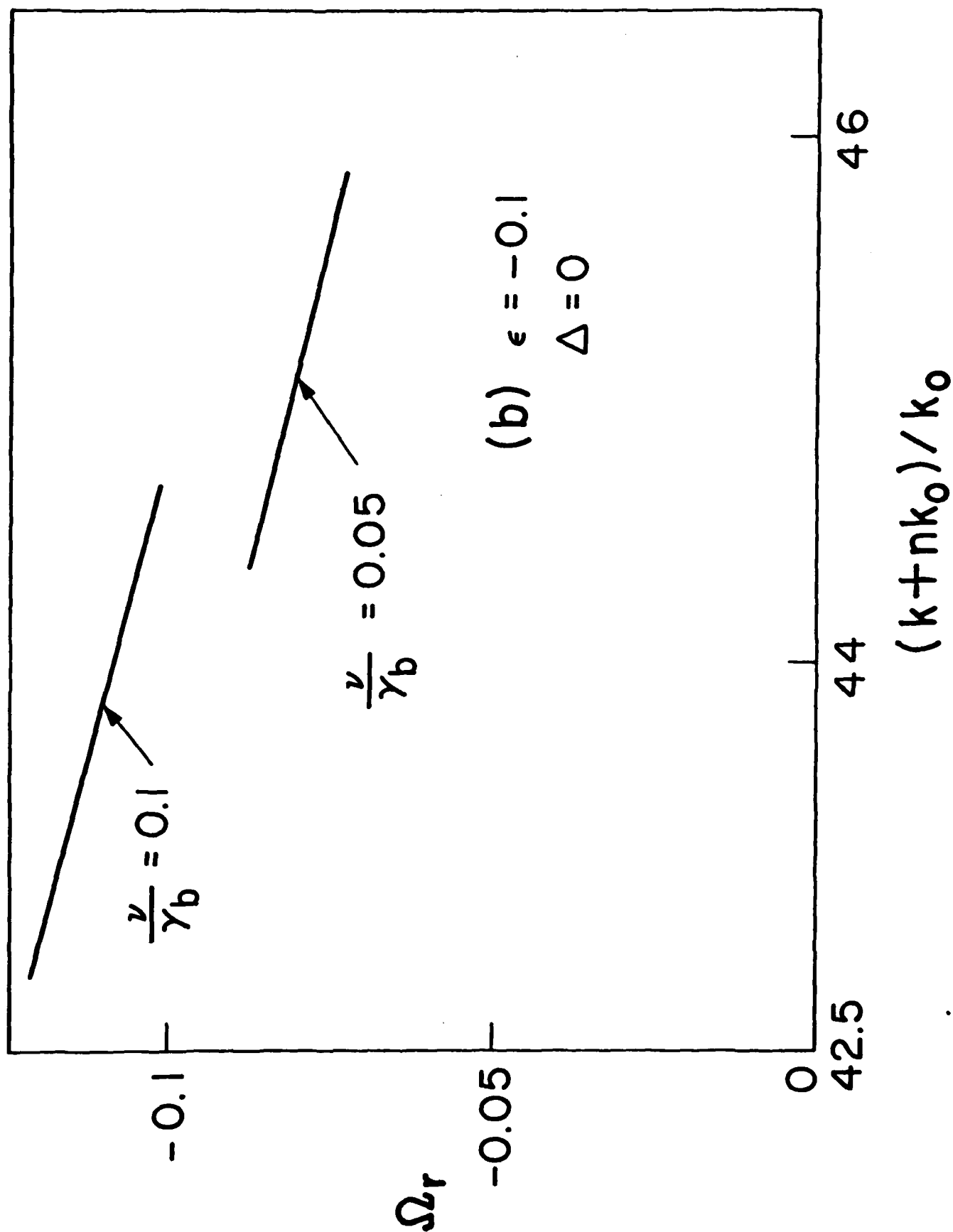
Fig. 1

Fig. 2

Fig. 3(a)

$\frac{\nu}{\gamma_b} = 0.1$

$\frac{\nu}{\gamma_b} = 0.05$

(b) $\epsilon = -0.1$

$\Delta = 0$

$(k+nk_0)/k_0$

Ω_r

-0.1

-0.05

0

42.5

44

46

Fig. 4(a)

(a) $\epsilon = 0.1, \Delta = 0$

$\frac{\nu}{\gamma_b} = 0.1$

$\frac{\nu}{\gamma_b} = 0.05$

$(k + nk_0)/k_0$

Ω_i

0.01

0.005

0

52   54   56

$$\frac{\nu}{\gamma_b} = 0.1$$

$$\frac{\nu}{\gamma_b} = 0.05$$

(b) $\epsilon = 0.1$
     $\Delta = 0$

Ω_r

$(k + nk_0)/k_0$

Fig. 4(b)

Fig. 5(a)

Fig. 5(b)